(Published in Acta Materialia **132**, 15 June 2017, Pages 367–373)

Effect of Nickel on point defects diffusion in Fe – Ni alloys

N. Anento[1], A. Serra[1] and Y. Osetsky[2*]

[1]Department of Civil and Environmental Engineering, E.T.S.E. Camins, Universitat Politècnica de Catalunya. Barcelona-Tech, Jordi Girona 1-3, 08034 Barcelona, Spain

[2]Materials Science and Technology Division, Oak Ridge National Laboratory, Oak Ridge, TN 37831-6138, USA

Abstract

Iron-Nickel alloys are perspective alloys as nuclear energy structural materials because of their good radiation damage tolerance and mechanical properties. Understanding of experimentally observed features such as the effect of Ni content to radiation defects evolution is essential for developing predictive models of radiation. Recently an atomic-scale modelling study has revealed one particular mechanism of Ni effect related to the reduced mobility of clusters of interstitial atoms in Fe-Ni alloys. In this paper we present results of the microsecond-scale molecular dynamics study of point defects, i.e. vacancies and self-interstitial atoms, diffusion in Fe-Ni alloys. It is found that the addition of Ni atoms affects diffusion processes: diffusion of vacancies is enhanced in the presence of Ni, whereas diffusion of interstitials is reduced and these effects increase at high Ni concentration and low temperature. The role of Ni solutes in radiation damage evolution in Fe-Ni ferritic alloys is discussed.

Keywords: diffusion, Fe-Ni alloy, radiation effects, molecular dynamics.

* Corresponding author e-mail: osetskiyyn@ornl.gov

1. Introduction

Vacancies and self-interstitial atoms (SIA) are point defects (PDs) profusely produced together with their clusters in materials under irradiation by energetic particles. Their evolution governs the degradation of materials properties, therefore theoretical and experimental studies have been devoted to elucidate the mechanisms that control the evolution of these defects under irradiation [1-8]. Many of the phenomena are controlled by atomic-scale mechanisms and atomistic modelling in many cases is the only technique that allows to study such mechanisms. For example, a multiscale study of radiation damage in Fe [9] has demonstrated how atomic-scale properties of PDs obtained by atomic level simulations such as *ab initio* and molecular dynamics (MD) modelling, used as input data for Monte-Carlo models, provide understanding of the experimentally observed resistivity recovery after electron irradiation. More extended defects and transport phenomena were also studied by atomic-scale modelling. Thus, stability and mobility of PD clusters in Fe, Cu and Zr were studied in [10,11] and the growth and shrinkage of clusters by the interaction with PDs were studied in pure Fe, Cu and Zr in [12-15]. One-dimensional diffusion of SIA clusters in bcc-Fe and fcc-Cu was reported in [16]. More recently extensive MD studies of the diffusion of single SIA and SIA clusters over a wide range of temperatures were performed in bcc-iron [17,18] using the modelling approach described in [19]. It was concluded that: i) the single SIA is a <110> dumbbell at all temperatures simulated and it migrates by a translation–rotation mechanism; ii) diffusion mechanism changes from the three-dimensional (3-D) to the one-dimensional (1-D) for clusters of 4–7 SIAs; iii) the activation energy of 1-D moving clusters is practically independent of the number of SIAs and does not exceed ~0.05eV. The 1-D migration of small interstitial clusters/dislocation loops, being an important mechanism of swelling under ion and neutron irradiation (see e.g. [3,4]), was studied in iron of different purities at room temperature under electron irradiation using a

high–voltage electron microscope [20,21]. The 1-D jump distance was found to be limited even in high-purity specimens and the distribution of jump distances was described by the distribution of the free path of interstitial clusters migrating through randomly distributed impurity atoms. The effect of impurities to 3-D migrating point defects and small clusters, especially of interstitial type, is undoubtedly important for the microstructure evolution under irradiation; however, it cannot be studied e.g. directly by electron microscopy.

A relevant alloying element in ferritic steels is Ni that, together with Cu and Mn, are considered to be the chemical elements mainly responsible for embrittlement in operation of reactor pressure vessels (RPV) at nuclear power plants. Meslin et al [22] showed that the role of Mn may be equally important than that of Ni in low-Cu RPV steels. Their concentration is explicitly included as a parameter in the empirical correlations describing the evolution of the radiation-induced ductile brittle transition temperature [23]. In addition, clusters observed in RPV steels contain as well Si and P solute atoms (see for instance, refs. [24-25]) that contributes to the embrittlement by segregating on grain boundaries and dislocations. So far, experimentally, not much is known about the role and mechanisms of Ni effects to the microstructure evolution. The first study addressing the effect of Ni exclusively was performed by Hoelzer and Ebrahimi [26] on the radiation-induced microstructure of pure Fe and Fe-0.7Ni. The damage consisted of <100> and 1/2<111> interstitial dislocation loops, whose size, number density and relative fraction was found to be affected by addition of Ni. While in pure Fe, 90% of the loops were of a<100> type, in the Fe-Ni alloy, the fraction of 1/2<111> loops was found to be 75%, but their number density increased and size decreased (approximately by a factor of two). These results agree with more recent experiments on pure Fe and RPV, irradiated by neutrons at ~300°C [27]. Unlike in pure Fe, a dense population of fine, hardly resolvable features was noticed in the alloys under two-beam dynamical imaging conditions. To elucidate the dynamics of point defects and small clusters in Fe-Ni alloys non-resolvable experimentally, MD simulations can be applied. In a recent publication [28] we presented results on SIA clusters

diffusion in Fe-Ni alloys with a wide range of Ni concentrations. A direct influence of Ni atoms to the 1-D glide and mobility of clusters was reported and the effects to microstructure evolution were discussed. In the present paper, we complete the study by reporting the results of extensive microsecond-scale MD modelling of 3-D diffusion by vacancy and interstitial atom mechanisms in Fe-Ni *ferritic* alloys with a variable Ni content.

The paper is organized as follows: in section 2 the modelling technique is described; in section 3 the parameters describing the diffusion of vacancies, SIAs and Ni atoms are presented. The discussion of results and conclusions are summarized in section 4.

2. Modelling technique

The diffusion of single point defects in Fe-Ni alloys has been studied using MD technique. Single interstitial atoms and vacancies performing 3-D diffusion were simulated in a cubic box with side length of ~4.57 nm containing N≈8000 mobile atoms. Vacancy diffusion was modelled in alloys with Ni concentrations of 0.8, 2.5 and 10 at.%. For the interstitial atom three additional Ni concentrations were considered: 0.5, 1.2 and 1.6 at.%. MD simulations were performed in the NVE ensemble with periodic boundary conditions in all directions. Atomic motion equations were integrated with the velocity-Verlet algorithm with time step in the range 1fs - 2.5fs depending on the temperature. Temperature range 300K - 900K was used for the interstitial diffusion and 600K -1400K for the vacancy. The equilibrium lattice parameter was fitted to ensure zero pressure conditions in all modelled cases.

The basic methods for MD diffusion data treatment used in this study were reviewed in [19] and applied in [17] for the study of diffusion in pure Fe. Three diffusion coefficients are considered, that related to the self-diffusion, D^*, and defect diffusion calculated using different approaches, D^d and D_v^d. D^* is calculated using the atomic square displacements (ASD) that can

be applied either to all atoms, R^2, giving the total alloy self-diffusion or matrix, R^2_{Fe}, and solute, R^2_{Ni}, atoms separately giving partial diffusion coefficients of each component:

$$D^* = \lim_{n\to\infty} \frac{< R^2(t) >}{2nt}$$

being n the dimensionality of the diffusion. If the simulated defect trajectory is long enough ASD is a linear function vs the simulated time and this linearity is the condition of applicability of this approach. Simulation over 1μs with trajectory output for every 10^3 time steps produces ~10^6 points on the ASD(t) dependence and the statistical treatment of these generates very low statistical error. Another advantage of this approach is that no defect detection is necessary which usually associates with additional computer resources and treatments.

Defect diffusion coefficient D_v^d can be estimated by jump frequency analysis (JFA). The JFA applies the atomistic theory of diffusion, namely there is a decomposition of the whole defect trajectory into separate jumps with a certain jump length, Δ, frequency, ν, and correlation factor, f_c:

$$D_v^d = f_C \frac{\nu \Delta^2}{2n}$$

The correlation factor is temperature and defect size/type dependent and can be calculated from the analysis of the jump directions:

$$f_C = \frac{(1+ < cos\ \theta >)}{(1- < cos\ \theta >)}$$

where $< cos\ \theta >$ is the mean cosine between the two consecutive jumps. This method of estimating defect diffusion coefficient works well if there are no long-range correlations in defects diffusion and therefore should be applicable for dilute alloys.

Alternatively, the defect diffusion coefficient D^d can be obtained by decomposing the defect trajectory into smaller segments of either equal time length (TTD) or equal number of jumps (TJD), estimating diffusion coefficient at each segment and then apply statistical average over all the segments. In TTD the trajectory of the defect is decomposed into isochronal segments

of duration t_{sd}, which is the parameter of the treatment method: it should be long enough to include all local correlations and the number of such segments should be large enough to provide statistically meaningful value of D^d when it is averaged over the whole trajectory [29]. For example, using TTD :

$$D^d = \frac{1}{N_{sd}} \sum_{i=1}^{N_{sd}} \frac{R_i^2}{2nt_{sd}}$$

where N_{sd} is the number of segments of t_{sd} duration. TJD is similar to TTD but here the decomposition is made by segments of the same number of jumps, J_{SD}. The main advantage of TTD and TJD techniques is the possibility to estimate a statistic accuracy of the estimated D^d and monitoring it to identify when modelling reaches the desired accuracy. Thus, if the defect trajectory is long enough, the value of D^d as a function of segment time in TTD or number of defect jumps in TJD converges to the value. Moreover, if there are no long-range correlations this value is the same as D_v^d described above (see e.g. [17, 19]).

In the present study all the above techniques have been used to cross-verify the accuracy of diffusion coefficients estimation. Tracer correlation factor, that indicates an efficiency of defect migration in atomic transport, was estimated as: $f_{tr} = \frac{D^*}{D^d}$.

Interatomic many-body potential for Fe-Ni interactions developed by Bonny *et al*. [30], was used in all presented simulations. This potential provides a good description of defect properties in the Fe-Ni alloy, e.g. the potential was fitted to DFT results for interaction energy of Ni–Ni and Ni–vacancy pairs and the binding energy for the mixed <110> dumbbell the pure Fe matrix [31]. For the Fe-Fe interactions we used the interatomic potential described in [32]. This interatomic potential was specially fitted to point defect properties in α-Fe. As in our previous work [17], the data we present here are obtained with a high statistical significance (up to $>10^5$ interstitial atom jumps and $\sim10^4$ vacancy jumps) by simulating a long physical time and using several independent simulations for the conditions where reasonable statistics of events

demands mesoscopic timespan. To attain enough statistics at the lower temperatures investigated, for which the jump frequency of the point defects is very low, several simulations were performed at the μs-scale (up to ~3μs).

The migration energy barriers of an interstitial atom and vacancy in the presence of Ni solute atoms in neighbouring positions were calculated using the molecular static technique in a system with N ≈ 12,000 atoms and the results are presented in table 1. The calculation of the energy barrier has been performed by constraining the relaxation of the displaced atom in the hyper-plane perpendicular to the vector connecting the initial and final positions.

3. Results

3.1. Vacancy diffusion

Self-diffusion coefficients, D^*, due to vacancy diffusion in all alloys studied are plotted in Fig.1a as a function of the inverse of temperature. The values of D^* practically overlap except for the Fe10at%Ni alloy which demonstrates a visual difference. For this alloy, we present Arrhenius plots of all the coefficients calculated: D^d, D_v^d and D^* in Fig.1b. A few features can be noted here:

1. Ni addition enhances self-diffusion and the effect increases at high Ni concentrations.
2. Vacancy diffusion coefficients calculated by TTD (diamonds) and TJD (triangles) methods are overlapped in the plot indicating a high accuracy in estimating diffusion coefficient values when both methods converge to the same value.
3. The vacancy diffusivity calculated by JFA (squares) practically overlaps with TTD and TJD at high temperatures and deviates towards higher values at low temperatures. This is because a large number of high frequency forward-backward vacancy jumps at lower temperatures do not contribute to its effective displacement. In other words, a simple estimation of jump correlation factor, f_c, by analysing angles between two consecutive jumps (see e.g.

[19]) is not accurate enough at low T when the number of such jumps increases due to a relatively strong vacancy-Ni attraction in the second coordination sphere (0.1eV, see [30]). We therefore use D^d values estimated by either TTD or TJD hereafter.

4. An Arrhenius plot for self-diffusion coefficients (circles) is below and practically parallel to the D^d plots (both TTD and TJD). This indicates that the tracer correlation factor is <1 and weakly dependent on the temperatures.

Among all the above diffusion coefficients the self-diffusion coefficient, D^*, is the most accurate for it is estimated directly from ASD without any assumptions on the defect motion. For an accurate estimation of Ni effects to the alloy diffusion we calculated the ratio of the alloy self-diffusion coefficient over the self-diffusion coefficient in pure Fe, $\frac{D^*_{FeNi}}{D^*_{Fe}}$. The results for different Ni concentrations are presented in Fig. 2a as a function of temperature. We notice that 10at.% of Ni increases twice the value of the diffusion coefficient at T=600K but the effect is weakening at higher temperatures and practically vanishes at T=1400K. Lower concentrations, namely, 0.8 and 2.5 at.%Ni present the same tendency but with lower values of the ratio. The activation energy of the vacancy diffusion (TTD) and self-diffusion by vacancy mechanism as a function of Ni concentration is presented in Table 2. In both cases the activation energy decreases when Ni concentration increases. The reduction in the activation energy along with the increase of diffusion coefficient indicates that mobility of both vacancies and atoms (mass transport) is *enhanced* in the presence of Ni in solid solution. This can be related to both, the above mentioned attractive interaction energy, 0.10eV, between the vacancy and the Ni atom at 2nd nearest neighbour (nn) and the reduced energy barrier for vacancy jumps near the Ni atom. Actually, the vacancy located at 2nd nn of Ni can jump into either an Fe atom located at 1st nn position of that Ni atom (energy barrier of 0.52eV) or to a Ni position located at 1st nn (energy barrier =0.61eV); in both cases the barrier is lower than in pure Fe (0.63eV) (see

Table 1). It is important to note that this reduction in the energy barrier is consistent with DFT calculations [31].

The tracer correlation factor for vacancy diffusion, f_{tr}, is plotted in Fig. 2b for all Ni concentrations including pure Fe as reference. The value of f_{tr} for a given defect is a measure of the efficiency of its migration in the atomic transport. The accuracy of f_{tr} calculations at low Ni concentrations is not enough to point out the Ni solute effect, however at 10 at.% the effect is considerable indicating strong correlations reducing the efficiency of migrating vacancy in producing atomic displacements, i.e. self-diffusion. However, the results reported provide enough evidences that in general, the presence of Ni solute atoms *accelerates* vacancy diffusion, *reduces* the diffusion activation energy and *enhances* the whole atomic transport due to the vacancy diffusion mechanism.

3.2 Interstitial atom diffusion

The self-diffusion coefficients for the interstitial atom diffusion in pure Fe and Fe-Ni alloys with 0.5, 0.8, 1.2, 1.6, 2.5 and 10at%Ni, estimated over the temperature range 300K-900K, are presented in Fig.3a. All dependences in Fig.3a are not linear and show different slope at low and high temperature indicating different activation energies. At high temperatures (T> 500K) the activation energy is almost not affected by Ni concentration, whereas at low temperatures (T< 500K) the influence of Ni concentration is remarkable. Thus, in the 10%Ni alloy the activation energy at low temperature is 0.38eV whereas at high temperature is 0.20eV. These values compare with the values for pure Fe reported in [17], i.e., 0.30 and 0.20eV respectively. In table 3 we have listed the average values per each concentration of Ni. In general, Ni effect in the interstitial atom diffusion is in the reduction of self-diffusion coefficient. This reduction increase at low temperature and high Ni content. This is clearly demonstrated in Fig.3b, where

the temperature dependence of the diffusion coefficient ratio, $\frac{D^*_{FeNi}}{D^*_{Fe}}$, is presented for different alloys. Actually, the ratio of self-diffusion coefficients *reduces* down to <0.2 when Ni concentration increases up to 10 at.% at 300K. In general, the presence of Ni solute atoms *reduces* all diffusion coefficients (Figs.3a and 3b), *increases* the diffusion activation energy (Table 3), *slows down* interstitial atom diffusion and the total atomic transport due to the interstitial diffusion mechanism. The decrease in the diffusion coefficient is due to the reduction in the jump frequency of the SIA, more effective at low temperature, related in turn to the negative binding energy of the SIA with the Ni atom. Thus, the jump asymmetry introduced by the repulsive interaction with Ni and the increase in backward jumps due to the instability of the mixt dumbbell causes the reduction on the SIA mobility.

The tracer correlation factor, f_{tr}, is plotted in Fig.3c for 0.8, 2.5 and 10 at.%Ni. We observe that, for all Ni concentrations, f_{tr} slightly differs from that in pure Fe indicating a weak Ni effect to the correlation between interstitial atom diffusion and total atomic mass transport.

3.3 Diffusion of Ni-solute atoms

Self-diffusion coefficients, D^*_{Ni}, of Ni in alloys were estimated by tracing the displacement of Ni atoms during the modelling of both, vacancy and interstitial atom diffusion. The corresponding Arrhenius plots for 0.8 and 10 at.% Ni concentrations are shown in Fig.4. Note that the partial diffusion coefficients presented for Fe-matrix and Ni-solute atoms are normalised per the corresponding component concentration. During modelling vacancy migration in Fe-0.8at.%Ni alloy at T=600K we did not observe significant displacements of Ni atoms over 2.8μs, therefore the corresponding diffusion coefficients are presented at Fig.4b only for T≥800K. Similar problems were observed in the estimation of Ni partial diffusion

coefficients by interstitial mechanism at low T (see Fig.4a). The activation energy of Ni atoms diffusion by both, vacancy and interstitial mechanisms obtained in the Arrhenius-type treatment (like the results in Figs.4) are presented in Table 4 together with the activation energies of point defects in pure Fe and the vacancy migration barrier for fcc Ni [30] for comparison. Table 1 indicates that, once a mixed dumbbell is created, the migration energy barrier is the same for the jump of Ni to form another mixed dumbbell as for the jump of Fe forming an SIA. Of course, the total energy balance is more favourable to the later event. Analysis of these results allows to note the following features:

1. In general, interstitial atoms diffusion is more efficient in transporting Ni atoms than that of vacancies and the difference increases significantly at lower temperatures.

2. Effects of Ni-solute atoms to interstitial and vacancy diffusion are opposite: *Ni accelerates vacancy diffusion and slows down interstitial diffusion.*

3. Ni-solute atoms transport is much slower than that of Fe-matrix atoms when interstitial diffusion occurs. On the contrary, for vacancy diffusion Ni- and Fe- atoms transport are practically the same.

4. In the case of vacancy diffusion mechanism, increasing Ni concentration leads to a decrease of all activation energies e.g. for vacancy diffusion and Ni-atoms diffusion. On the contrary, in the case of interstitial diffusion mechanism addition of Ni increases all these activation energies.

Visual analysis of solute atoms diffusion has shown the usual mechanisms of solute transport, i.e. exchange vacancy-Ni jumps for the vacancy diffusion mechanisms and formation of a mixed Fe-Ni <110> dumbbell for the interstitial diffusion mechanism. Migrating vacancy spends more time as a vacancy-Ni complex than in the isolated Fe site. This is because the binding energy of a vacancy in the second neighbour position on Ni atom in Fe matrix is rather attractive, 0.10eV. Vacancy spends some time in this position jumping out or to the first nearest

neighbour position (with a weak repulsion, -0.02eV) and returning. Due to these return jumps vacancy correlation factor decreases although vacancy keeps the ability to displace Ni atoms quite effectively. Such a specific behaviour of vacancy-solute binding energy i.e. a weak repulsion in the nearest neighbour and much stronger attraction in the second neighbour, is qualitatively consistent with DFT calculations in the bcc Fe-Ni system and also leads to a vacancy drag mechanism for Ni transport as was demonstrated in [33] by a combination of mean field with DFT derived defect migration barriers. We therefore expect that in our MD modelling Ni transport also occurs by vacancy drag mechanism although we did not estimate transport coefficients here.

The interaction between an interstitial atom and Ni-solute affects strongly the interstitial diffusion mechanism. The binding energy of a Ni atom with SIA <110> dumbbell is repulsive and depends on the relative position of the Ni atom, i.e. -0.14eV and -0.12eV when it is in the tensile region and compressive region, respectively [30]. Despite the binding energy of the mixed Fe-Ni <110> dumb-bell is quite repulsive, -0.35eV [30], in good agreement with DFT calculations [31], there is experimental evidence of its formation [34]. One would expect a low probability to form mixed dumb-bells and therefore a very low efficiency of interstitial diffusion mechanism in providing Ni-atoms transport. In principle, this is what we have observed and atomic displacements of Ni-atoms (event normalised per their concentration) and, therefore, the tracer diffusion coefficient, D^*_{Ni}, are a few times lower than those of Fe-atoms as seen in Fig.4a. Moreover, we almost did not observe formation of mixed dumb-bells, and therefore Ni atoms transport, at low T where the repulsion effect is maximum. At high enough T mixed dumb-bells were formed providing therefore displacements of Ni-solute atoms. Since there is not attraction between interstitial configuration and Ni-solute there are no correlation effects as to vacancy described above. This is consistent with the results presented in Fig.3c where practically no Ni-effect to tracer correlation factors was pointed out.

5. Discussion and concluding remarks

The transport properties due to vacancy and interstitial atom diffusion in Fe-Ni alloys were studied using microsecond-scale molecular dynamics. This work is an extension of our previous study of interstitial clusters mobility in Fe-Ni alloys [28] where it was demonstrated that Ni impurities slowdown one-dimensional glide of interstitial clusters up to complete immobilization of large clusters or in high Ni content alloys. Complete damping of 1-D glide mechanism reduces or even prevents completely the so called production bias [3, 4, 28] which is a powerful mechanism of swelling under neutron and ion irradiation. In addition, damping 1-D glide increases a concentration of interstitial clusters /dislocation loops left in the bulk. In the present work we report the effect of Ni to the 3-D mobility of point defects and the possible consequences of this.

First, the Ni effect to 3-D mobility of point defects is significantly weaker than the found in [28] effect to the 1-D glide.

Second, Ni-solute atoms affect both vacancy and interstitial diffusion. The effects are opposite: for vacancy diffusion is accelerated (see Figs.1 and 4) whereas interstitial diffusion is decelerated in the presence of Ni-atoms (see Figs.3 and 4). The effect is stronger for the interstitial mechanism and weaker for the vacancy one. In general we conclude that Ni effects to 3-D diffusion studied here enhance more the effects to 1-D glide of interstitial clusters reported earlier [28]. Thus, acceleration of vacancy diffusion together with deceleration of interstitial atom diffusion should affect the swelling behaviour due to a) decreasing the *conventional dislocations bias* (i.e. creating vacancy supersaturation due to preferential absorption of interstitial atoms on edge dislocations) and b) increasing *recombination* of vacancies and interstitial atoms in the bulk. The results on point defects and cluster mobility in Fe-Ni alloys obtained here and in [28] used in mesoscale and continuum modelling will allow

to obtain qualitatively new and quantitative more accurate results on microstructure evolution under irradiation.

And finally third, the enhanced mobility of Ni-atoms by vacancy mechanism should affect the alloys phase transformation and segregation under irradiation. Thus, the pressurized water reactors at Ringhals, Sweden, with low copper and phosphorus content but anomalously high concentration of manganese and nickel, $\gtrsim 1.6\%$, in the welds [24], appear to brittle more severely than expected [24, 25]. The reason for this is likely to be the enhanced formation of large volume fraction of nickel-manganese precipitates observed by APT [25, 35]. These elements are suspected to agglomerate by segregating on previously formed point-defect clusters, transported by diffusion of point defects. Based on this mechanisms Chiapetto et al [36] have applied an OKMC model to predict the microstructure evolution of the RPV steel from the Ringhals reactors. In their model the presence of impurities such as Mn and Ni is treated with a "grey-alloy" approach, i.e. the solute atoms are not explicitly present in the simulation system, but their effect is introduced by modifying the mobility parameters that characterize point defects (both interstitial and vacancy) and their clusters. They report that even such a simple “grey-alloy” approach allows to identify the qualitatively correct trends in terms of defects density and average size as compared to the experimental material characterization. The explicit accounting of solute transport by atomic-scale mechanisms studied in the present work would be a step forward in the accurate description of the microstructure evolution.

Disclaimer

This paper reflects only the author's view. The European Commission is not responsible for any use that may be made of the information it contains.

Acknowledgements

This project has received funding from the Euratom research and training programme 2014-2018 under grant agreement No 661913 (SOTERIA) and contributes to the Joint Program on Nuclear Materials (JPNM) of the European Energy Research Alliance (EERA). This work was partly supported by the Energy Dissipation to Defect Evolution (EDDE), an Energy Frontier Research Center funded by the U.S. Department of Energy, Office of Science, Basic Energy Sciences (YNO) and partly by the Spanish MINECO (FIS2015-69017-P) (NA & AS)

References

1. S.L. Dudarev, J.L. Boutard, R. Lässer, M.J. Caturla, P.M. Derlet, M. Fivel, et al., The EU programme for modelling radiation effects in fusion reactor materials: An overview of recent advances and future goals, J. Nucl. Mat. 386–388 (2009) 1-7.

2. B.N. Singh, Void Volume Swelling dependent on Grain Size in an Austenitic Stainless Steel, Nature 244 (1973) 142-142.

3. B.N. Singh , S.I. Golubov, H. Trinkaus, A. Serra, YuN Osetsky, A.V. Barashev, Aspects of microstructure evolution under cascade damage conditions, J.Nuc. Mater. 251 (1997) 107-122.

4. S.I. Golubov, A.V. Barashev, R.E. Stoller, Radiation damage theory, in: R.J.M. Konings (Ed.), Comprehensive Nuclear Materials, vol. 1, Elsevier, Amsterdam, 2012, pp. 357–391.

5. S.J. Zinkle, K. Farrell, Void swelling and defect cluster formation in reactor-irradiated copper, J. Nucl. Mater. 168 (1989) 262-267.

6. S.I. Golubov, A.V. Barashev, R.E. Stoller, B.N. Singh, Breakthrough in understanding radiation growth of zirconium, in: R.J. Comstock (Ed.), Proceedings of 17th International Symposium “Zirconium in the Nuclear Industry”, ASTM STP 1543, ASTM International, West Conshohocken, PA, 2014, pp. 729–758.

7. M. Kiritani, Proc. Int. Conf. on High Voltage Electron Microscopy, Antwerp 1980, p.196.

8. M. Kiritani, Defect interaction processes controlling the accumulation of defects produced by high energy recoils, J. Nucl. Mater. 251 (1997) 237-251.

9. C.C. Fu, J. Dalla Torre, F. Willaime, J.L. Bocquet and A. Barbu, Multiscale modelling of defect kinetics in irradiated iron, Nature Mater. 4 (2004) 68-74.

10. Yu. N. Osetsky, D.J. Bacon, A. Serra, B.N. Singh, S.I. Golubov, Stability and mobility of defect clusters and dislocation loops in metals, J. Nucl. Mater. 276 (2000) 65-77.

11. N. de Diego, A. Serra, D.J. Bacon,Y. N. Osetsky, On the structure and mobility of point defect clusters in alpha-zirconium: a comparison for two interatomic potential models, Modelling Simul. Mater. Sci. Eng 19 (2011) 035003 (11pp).

12. M. Pelfort, Y.N. Osetsky, A. Serra, Vacancy interaction with glissile interstitial clusters in bcc metals , Philos. Mag. Let. 81 (2001) 803-811.

13. M.A. Puigvi, Y.N. Osetsky, A. Serra, Interactions between vacancy and glissile interstitial clusters in iron and copper, Mater. Sci. Eng. A365 (2004) 101-106.

14. M.A. Puigvi, N. de Diego, A. Serra, Y.N. Osetsky, D.J. Bacon, On the interaction between a vacancy and self-interstitial atom clusters in metals, Philos. Mag. 87 (2007) 3501-3517.

15. N. Anento, A. Serra, Interaction of a single interstitial atom with small clusters of self interstitials in α-Fe, J. Nucl. Mater. 372 (2008) 239-248.

16. Y.N. Osetsky, D.J. Bacon, A. Serra, B.N. Singh, S.I. Golubov, One-dimensional atomic transport by clusters of self-interstitial atoms in iron and copper, Philos. Mag. 83 (2003) 61-91.

17. N. Anento, A. Serra, Y.N. Osetsky, Atomistic study of multimechanism diffusion by self-interstitial defects in α-Fe, Model. Simul. Mater. Sci. Eng. 18 (2010) 025008 (18pp).

18. D.A. Terentyev L. Malerba, M. Hou, Dimensionality of interstitial cluster motion in bcc-Fe, Phys. Rev. B 75 (2007) 104108 (13pp).

19. Y.N. Osetsky, Defects and Diffusion in Metals - Annual Retrospective III, *Defect and Diffusion Forum*, 188-190 (2003) 71.

20. Y. Satoh, H. Matsui, T. Hamaoka, Effects of impurities on one-dimensional migration of interstitial clusters in iron under electron irradiation, Phys. Rev. B 77 (2008) 094135 (10pp).

21. Y. Satoh and H. Matsui, Obstacles for one-dimensional migration of interstitial clusters in iron, Philos. Mag. 89 (2009) 1489-1504.

22. E. Meslin, B. Radiguet, M. Loyer-Prost, Radiation-induced precipitation in a ferritic model alloy: An experimental and theoretical study, Acta Mater. 61 (2013), 6246–6254

23. ASTM Standard E 900, 2002 2007 *Predicting Radiation-Induced Transition Temperature Shift in Reactor Vessel Materials, E706 (IIF)* (West Conshohocken, PA: ASTM International) www.astm.org.

24. P. Efsing, C. Jansson, G. Embring, and T. Mager, "Analysis of the Ductile-to-Brittle Transition Temperature Shift in a Commercial Power Plant with High Nickel Containing Weld Material, J. ASTM Int. 4 (2007) 1–12.

25. M.K.Miller, K. A. Powers, R. K. Nanstad, and P. Efsing, Atom probe tomography characterizations of high nickel, low copper surveillance RPV welds irradiated to high fluences. J. Nucl. Mater. 437 (2013) 107-115.

26. D.T. Hoelzer, F. Ebrahimi, Effect of Copper and Nickel on the Neutron Irradiation Damage in Iron Alloys, Mat. Res. Soc. Symp. Proc. 373 (1995) 57.

27. M. Hernandez-Mayoral, D. Gomez-Briceno, Transmission electron microscopy study on neutron irradiated pure iron and RPV model alloys, J. Nucl. Mater. 399 (2010) 146-153.

28. Y.N. Osetsky, N. Anento, A. Serra, D. Terentyev, The role of nickel in radiation damage of ferritic alloys, Acta Mater. 84 (2015) 368–374.

29. M.W. Guinan, R.N. Stuart, R.J. Borg, Fully dynamic computer simulation of self-interstitial diffusion in tungsten, Phys. Rev. B 15 (1977) 699-710.

30. G. Bonny, R.C. Pasianot, L. Malerba, Fe–Ni many-body potential for metallurgical applications, Modelling Simul. Mater. Sci. Eng. 17 (2009) 025010 (13pp)

31. E. Vincent, C.S. Becquart, C. Domain, Ab initio calculations of vacancy interactions with solute atoms in bcc Fe, Nucl. Instr. Methods Phys. Res. B 228 (2005) 137-141; Atomic kinetic Monte Carlo model based on ab initio data: Simulation of microstructural evolution

under irradiation of dilute Fe–CuNiMnSi alloys, Nucl. Instr. Methods Phys. Res. B 255 (2007) 78-84.

32. M.I. Mendelev, A. Han, D.J. Srolovitz, G.J. Ackland, D.Y. Sun, M. Asta, Development of new interatomic potentials appropriate for crystalline and liquid iron, Phil Mag 83 (2003) 3977-3994.

33. L.Messina, M.Nastar, T. Garnier, C. Domain and P. Olsson, Phys. Rev. B 90 (2014) 104203

34. FMaury, A. Lucasson, P. Lucasson, P. Moser and F. Faudot, Interstitial migration in irradiated iron and iron-based diluted alloysJ. Phys.: Condens. Matter 2 (1990) 9291-9307.

35. P.D.Styman, J. M. Hyde, D. Parfitt, K. Wilford, M. G. Burke, C. A. English, and P. Efsing, Post-irradiation annealing of Ni–Mn–Si-enriched clusters in a neutron irradiated RPV steel weld using Atom Probe Tomography J. Nucl. Mater. 459 (2015) 127-134.

36. M. Chiapetto, L. Messina, C.S. Becquart, P. Olsson, L. Malerba, Nanostructure evolution of neutron-irradiated reactor pressure vessel steels: revised Object kinetic Monte Carlo model, COSIRES 2016 Proc. in Nuc. Instr. Methods Phys. Res B, 393, (2017)105-109

FIGURES

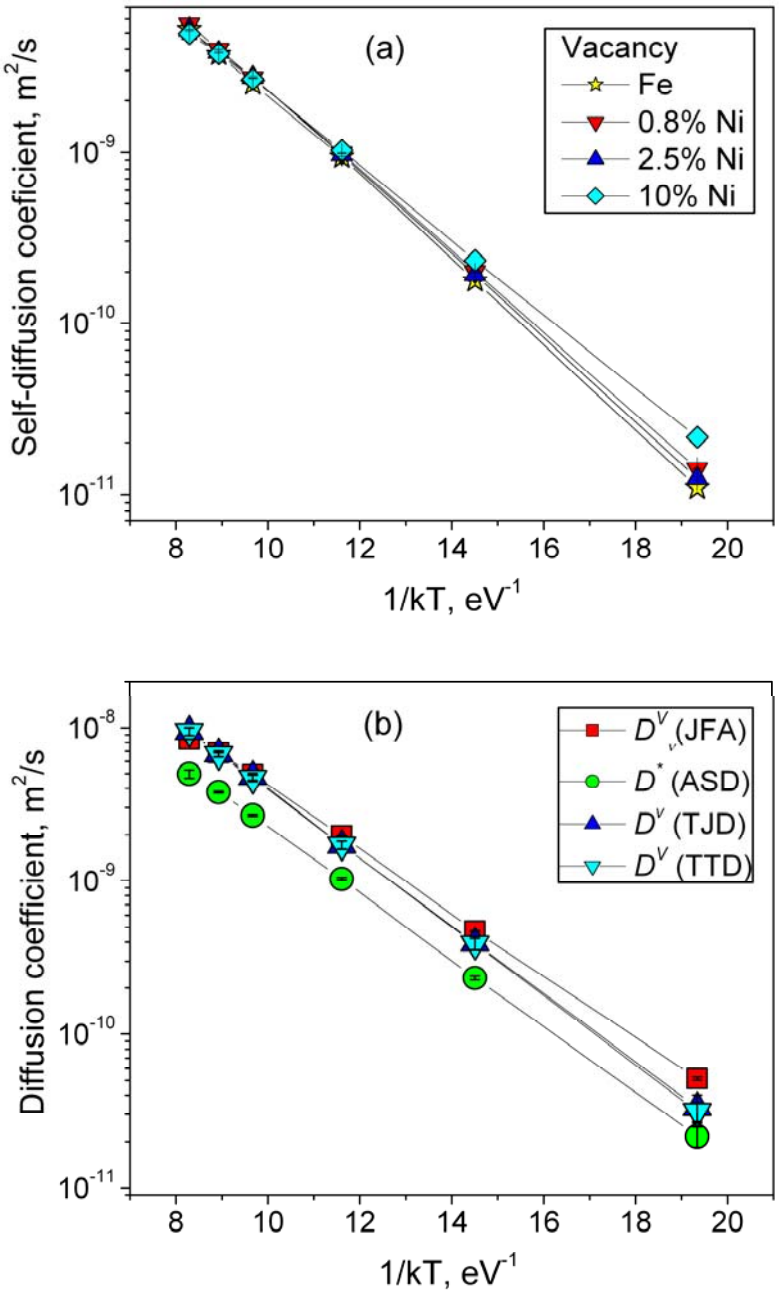

Figure 1. (a) Self-diffusion coefficient D* versus T^{-1} for the single vacancy in pure Fe and Fe-Ni alloys. (b) Defect diffusivity and self-diffusion coefficients versus T^{-1} for the single vacancy in Fe-10%Ni alloy.

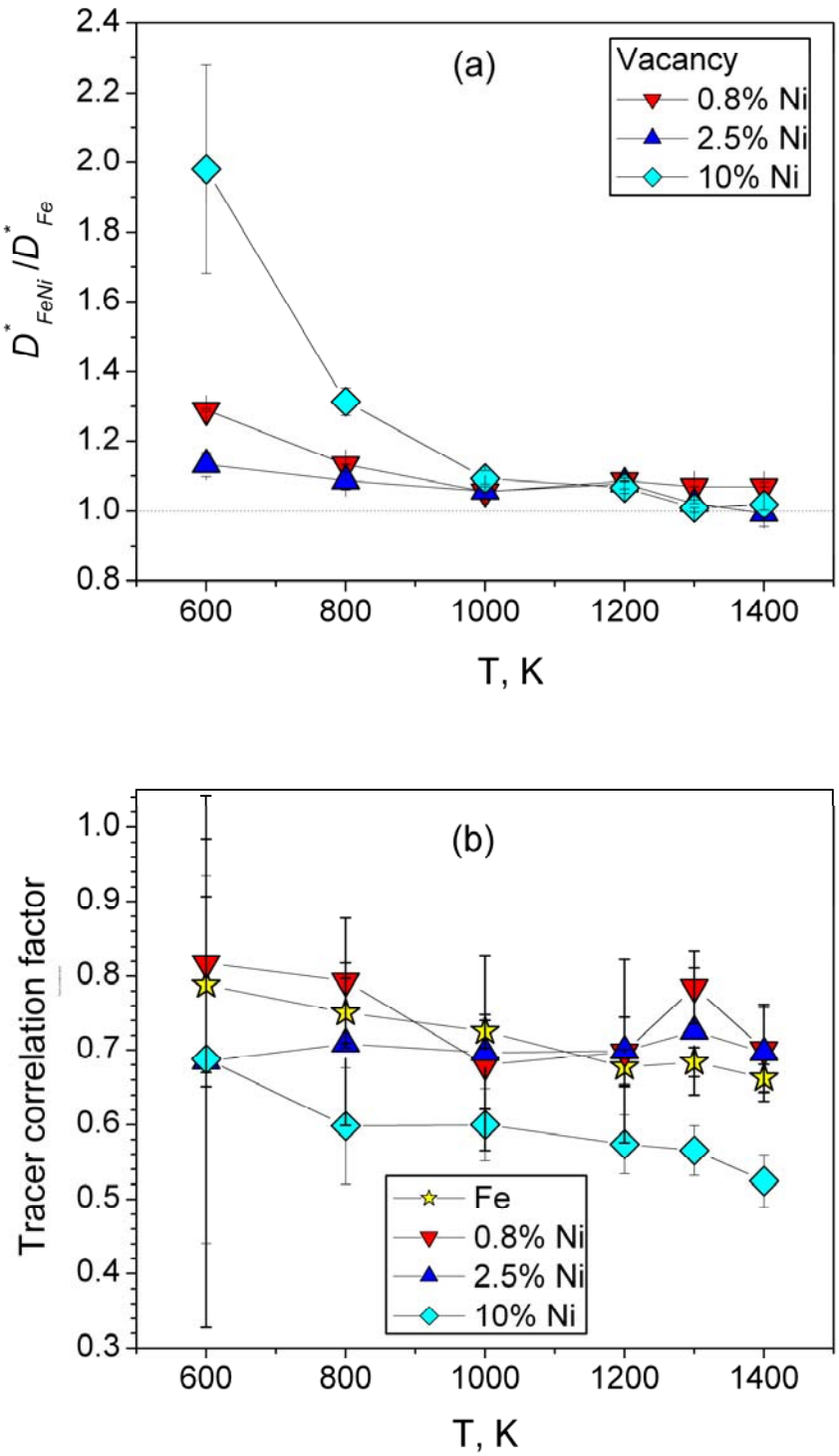

Figure 2. (a) Ratio of self-diffusion coefficients $\frac{D^*_{FeNi}}{D^*_{Fe}}$ versus T obtained for the vacancy diffusion mechanism in different alloys. (b) Tracer correlation factor for the single vacancy for all Ni concentrations.

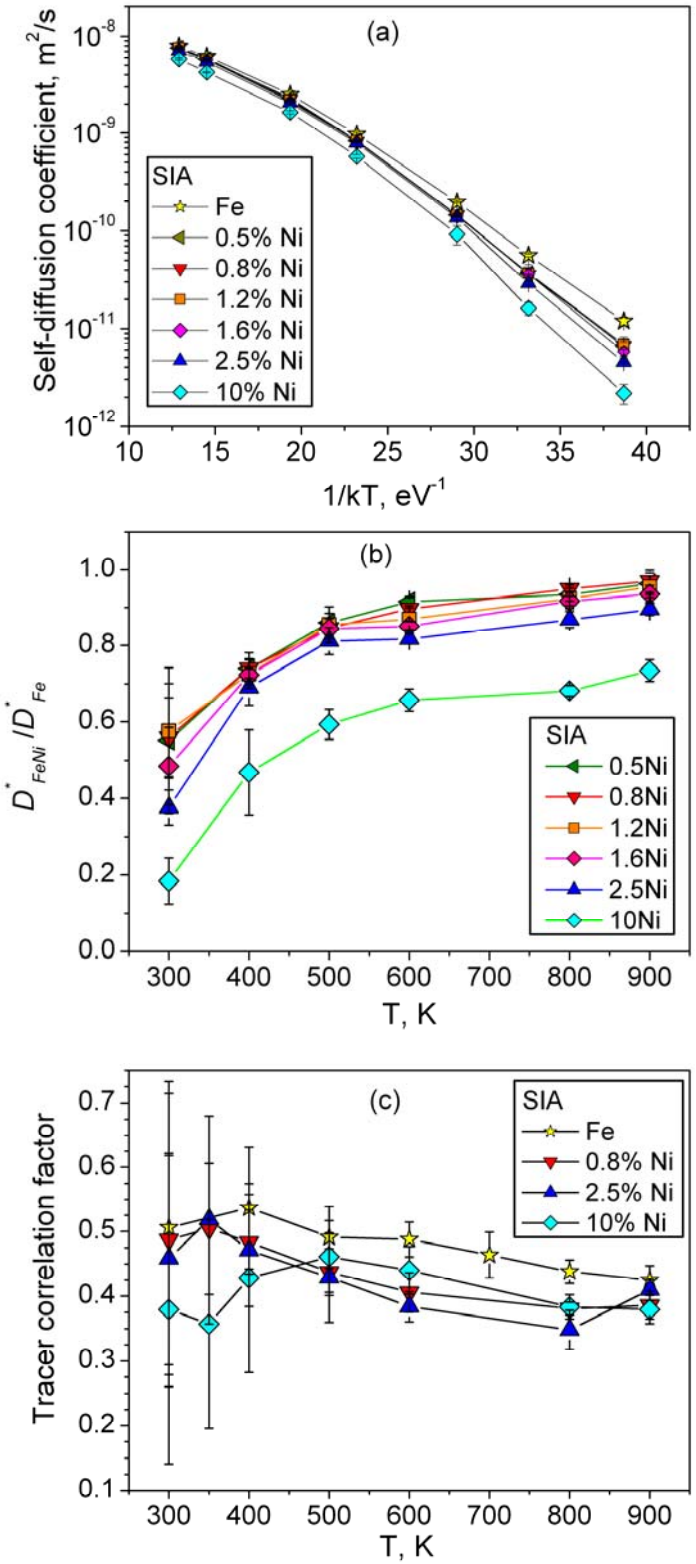

Figure 3. (a) Self-diffusion coefficient D* versus T^{-1} for the single SIA in pure Fe and Fe-Ni alloys. (b) Ratio of self-diffusion coefficients $\frac{D^*_{FeNi}}{D^*_{Fe}}$ versus T obtained for the interstitial diffusion mechanism in different alloys. (c) Tracer correlation factor for the single SIA for all Ni concentrations.

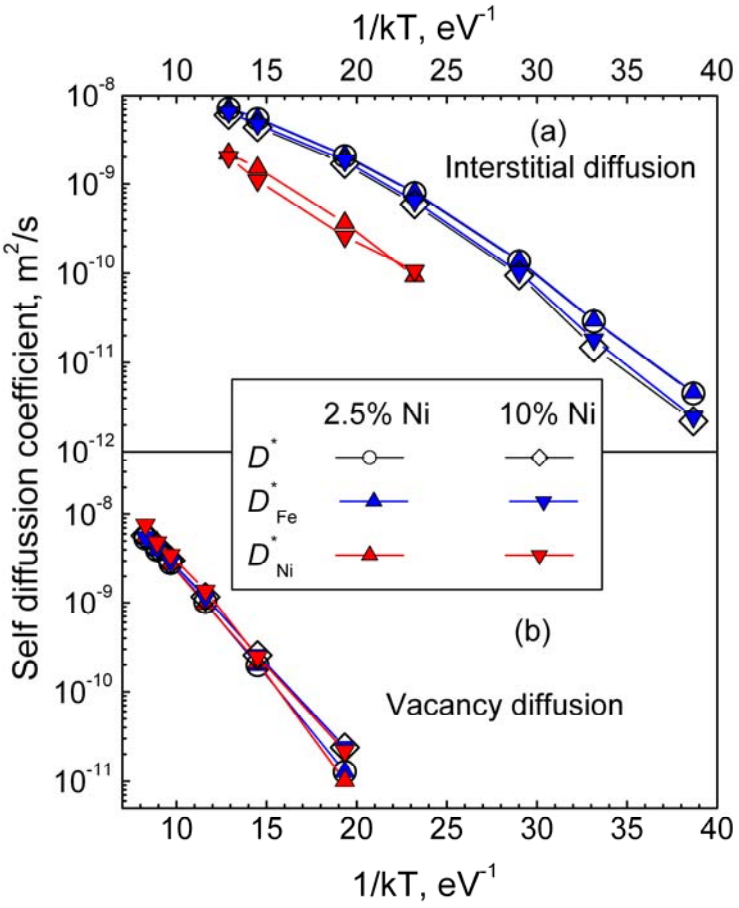

Fig.4 Self-diffusion coefficients for Fe-0.8at.%Ni and Fe-10at.%Ni alloys, D^*, and its components, D^*_{Fe} and D^*_{Ni} versus T^{-1} estimated for (a) interstitial atom and (b) vacancy diffusion mechanisms. Note that the components diffusion coefficients are normalised per their concentration.

TABLES

Table 1. Energy barriers in eV for elementary jumps of different type around vacancy and interstitial atom in Fe matrix with Ni impurity. If there is asymmetry in the jump, the backward jump energy is indicated. The values with * symbol are obtained from reference [30]. For the vacancy migration it is indicated which atom is jumping (Fe or Ni). We have also considered migration of the vacancy with a solute on the vicinity; E_m(Fe, Ni Xnn): the solute atom is X^{th} neighbour of the Fe atom before jumping.

Vacancy migration energy barrier (eV)		SIA migration energy barriers (eV)	
Fe	0.63*	Fe-Fe (bulk)	0.31
Ni	0.61*	Fe-Fe Ni(1nn) tension Backward jump	0.35 0.34
Fe, Ni 2nn	0.52*	Fe-Fe Ni(1nn) compres. Backward jump	0.23 0.33
Fe, Ni 3nn	0.71*	Fe-Ni to Ni-Fe	0.13
Fe, Ni 5nn	0.68*	Ni-Fe to Fe-Fe Backward jump	0.13 0.37

Table 2. Activation energy for the single vacancy calculated by two different methods (eV).

alloy	Activation energy for vacancy diffusion mechanism (eV)	
	Vacancy diffusion (TTD)	Self-diffusion (ASD)
Fe	0.57	0.56
Fe-0.8%Ni	0.55	0.54
Fe-2.5%Ni	0.54	0.55
Fe-10%Ni	0.52	0.50

Table 3. Averaged activation energy for the single SIA calculated by two different methods (eV).

alloy	Activation energy for interstitial diffusion mechanism (eV)	
	Interstitial diffusion (TTD)	Self-diffusion (ASD)
Fe	0.27	0.26

Fe-0.8%Ni	0.28	0.27
Fe-2.5%Ni	0.29	0.28
Fe-10%Ni	0.29	0.31

Table 4. Activation energy in eV for Ni atoms in Fe-Ni alloys for different diffusion mechanisms as a function of Ni impurity concentration. Data for pure Ni and Fe are also presented for comparison.

Ni concentration, at.%	Activation energy for Ni diffusion (eV)	
	Mechanism	
	Vacancy	Interstitial
0.8	0.62	0.34
2.5	0.57	0.31
10	0.53	0.28
fcc Ni	0.98 [30]	0.13
bcc Fe	0.56	0.26